

Hierarchical Design of Continuous Line Illustrations

Fernando J. Wong and Shigeo Takahashi

The University of Tokyo, Tokyo, Japan
{fjwong, shigeo}@visual.k.u-tokyo.ac.jp

Keywords: Line Illustration, Hierarchical Design, Eulerian Paths.

Abstract: A hierarchical approach for designing continuous line illustrations, drawings that consist of a single line, is presented throughout this paper. Users specify a graph that will guide the overall shape of the line illustration, and proceed to assign a series of child graphs to many of its vertices. A line illustration can then be generated by taking all of these graphs into account, allowing us to produce complex drawings that are composed of several objects. Our approach also allows us to preserve the overall structure and orientation of the line as graphs are inserted or removed from the illustration. We also propose a variety of visual enhancements for our illustrations based on the specified hierarchical graph information and provide several result examples that demonstrate the effectiveness of our approach.

1 INTRODUCTION

Continuous Line Illustrations (CLI) are a subclass of artistic drawings that abstract an object or scene with a single line that portrays the most relevant features of the object in question. This style is often taught in art courses as a technique to help students develop their artistic senses (Nicolaïdes, 1990). Apart from artistic purposes, CLIs also have many real-world applications in the production of quilting designs (Fritz, 2001), steel wire sculptures (Lohman, 2009), and connect-the-dots puzzles, just to name a few.

Despite their simple nature, there is actually quite a variety of CLI styles. For example, the works of Morales (Morales, 2005) consist of a non-intersecting line of uniform thickness, which approximates the shading of the scene through the variation of line density at different areas. Slater’s paintings (Slater, 2001) depict a non-intersecting line that varies in thickness and color accordingly, covering most of the canvas with the line while beautifully portraying the color of the scene. In Lindsay’s works (Lindsay, 2010), a self-intersecting smooth curve with uniform thickness is traced, while often portraying several objects along the line. Sable’s drawings (Sable, 2009) also contain several self-intersections in them, while adding variations in line thickness accordingly, in order to achieve shading effects with the line.

Our work aims to provide a framework for generating CLIs of individual objects (Figures 1(a), 1(b) and 1(c)), as well as designing complex CLIs con-

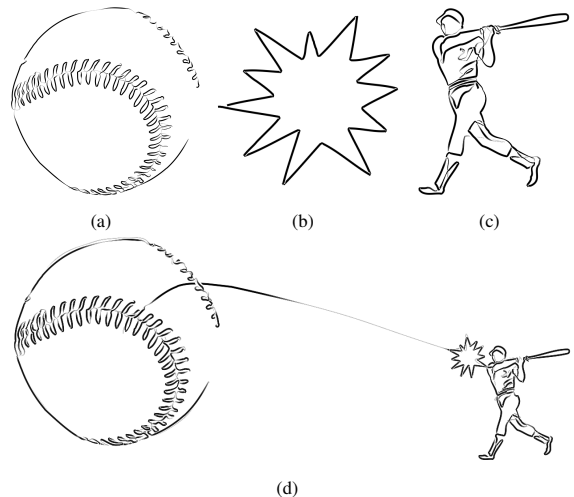


Figure 1: (a,b,c) Continuous line illustrations of individual objects. (d) Different objects can be combined in order to produce more complex illustrations.

taining several parts (Figure 1(d)). Previous works addressed the image-based automatic generation of CLIs, while no research has been conducted thus far on how to design such complex illustrations.

This paper is organized as follows: Previous works relevant to our research are presented in Section 2. An overview of our hierarchical CLI approach is provided in Section 3, and further details are given throughout Sections 4, 5 and 6. Results of our approach are discussed in Section 7, followed by conclusions and pointers to future work in Section 8.

2 RELATED WORK

As was mentioned earlier, previous works focused on the automatic generation of CLIs from input images. The first of these works was given in (Bosch and Herman, 2004), where a continuous line drawing was created by first obtaining a point distribution based on the image intensity, and then solving an instance of the traveling salesman problem (TSP) over the set of points. This approach was later extended in (Kaplan and Bosch, 2005) by making use of modern image stippling techniques, in order to obtain a point distribution that better approximated the image. These works aimed to produce CLIs that resembled the appearance of Morales' works (Morales, 2005), achieving a type of half-toning technique based on a non-intersecting continuous line. Work on how to generate self-intersecting CLIs that portray the contours of the image instead of its shading was proposed recently in (Wong and Takahashi, 2011). In this approach, a graph is created from edges detected in the image, and then a CLI is modeled after an Eulerian path in this graph, resulting in illustrations that are more similar in nature to those of Lindsay (Lindsay, 2010). Our work builds up on this last approach for creating line illustrations that portray several objects.

CLIs also share a relationship with labyrinths and mazes. For example, the labyrinth-like structures proposed in (Pedersen and Singh, 2006) are, in essence, CLIs as well. Their method is based on the evolution of curves into an organic labyrinth pattern, through the iterative application of forces. CLIs can also be found in the solutions of picture mazes. The method in (Wong and Takahashi, 2009) introduced an iterative cycle growing and merging procedure for creating maze solution paths that approximated the shape and shading of an image.

3 METHOD OVERVIEW

The proposed framework takes a set of graphs as input, which represent the many objects or silhouettes that will compose the final line illustration (Figures 2(a), 2(b) and 2(c)). In order to create these graphs, our prototype system allows users to provide a number of images in order to automatically derive a graph from each of them as described in (Wong and Takahashi, 2011). Alternatively, users can design their own graphs by tracing rough sketches, after which our system will derive the graphs from them. Users then specify one of these graphs as a root graph (Figure 2(b)), and assign a series of child graphs to any of its vertices with a click of the mouse (Fig-

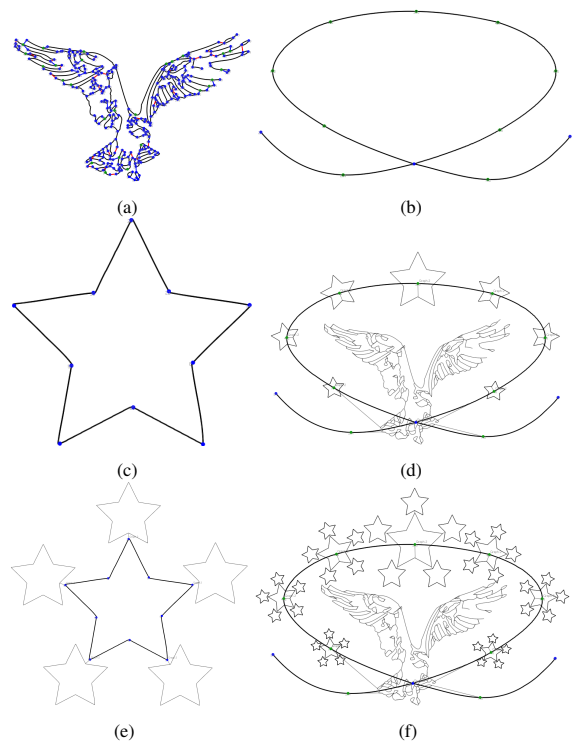


Figure 2: Method overview. (a,b,c) A set of basis graphs is specified by the user. These graphs can be either (a) image-derived or (b,c) user-generated. (b) A root graph is designated, and (d) several child graphs are assigned to its vertices. (e) A child graph can also contain its own set of children. (f) Moreover, a child graph can be referenced by different vertices of its parent, automatically propagating any changes in the child graph to all vertices pointing to it.

ure 2(d)). Child graphs can also contain their own set of children in order to portray more complex objects (Figure 2(e)), and they can also be translated, rotated or scaled relative to their parents.

After the graph assignment phase, a CLI is generated in a top-down manner, starting with the root graph and then proceeding with the graphs located at deeper levels. We attempt to preserve the coherence of the CLI across hierarchical levels, that is, assigning a child graph to a vertex should only affect the shape of the final CLI at that location, but have no impact on the endpoints nor on the orientation of the CLI as a whole. Also, we exploit the hierarchical relationships between the graphs in order to achieve a variety of visual effects along the line.

4 HIERARCHICAL CLI DESIGN

As mentioned earlier, our system generates CLIs composed of several objects by specifying hierarchi-

cal relationships between different graphs that represent each of these objects. In this section, we describe the underlying structure used to model these hierarchical relations in our line illustrations.

4.1 The Hierarchical Graph

The input to our framework is a set of user-specified **basis graphs** $\mathbf{G} = \{G_1(V_{G_1}, E_{G_1}), \dots, G_n(V_{G_n}, E_{G_n})\}$, where V_{G_i} and E_{G_i} are the sets of vertices and edges of graph G_i , respectively. The relationship between these graphs is modeled as a directed graph $H(V_H, E_H)$, which we refer to as the **hierarchical graph** of the CLI (Figure 3). Each vertex $h \in V_H$ contains a pointer to a basis graph $G(h) \in \mathbf{G}$, while each directed edge $e_h = (h_p, h_c) \in E_H$, between a **parent vertex** h_p and a **child vertex** h_c , encodes information needed in order to model the relationship between the **parent graph** $G(h_p) \in \mathbf{G}$ and the **child graph** $G(h_c) \in \mathbf{G}$. The information stored in each edge $e_h \in E_H$ includes:

- The position, rotation angle and scaling of $G(h_c)$ relative to $G(h_p)$.
- A pair of endpoint vertices $v_p(e_h) \in V_{G(h_p)}$ and $v_c(e_h) \in V_{G(h_c)}$, through which $G(h_p)$ and $G(h_c)$ are connected.
- The type of relation established between $G(h_p)$ and $G(h_c)$ (Section 4.2).

We allow any number of edges $e_h = (h_p, h_c) \in E_H$ between any two vertices $h_p, h_c \in V_H$ as seen in Figure 3. In other words, a parent graph $G(h_p)$ can be assigned the same child graph $G(h_c)$ at many of its vertices. This allows us to modify $G(h_c)$ by assigning its own set of children to it, and have the changes be automatically reflected in all other vertices in $G(h_p)$ that also have a reference to $G(h_c)$ (Figure 2(f)).

4.2 Hierarchical Relation Types

Users can specify one of two relation types between parent and child graphs: **single link** and **multiple link** relations. In single link relations, a child graph is connected to its parent by inserting a **linking edge** that connects a vertex $v_c(e_h)$ in $G(h_c)$ directly with another vertex $v_p(e_h)$ in $G(h_p)$. In multiple link relations, several linking edges are inserted between the neighbors of $v_p(e_h) \in G(h_p)$ and a number of vertices in $G(h_c)$, one for each neighbor of $v_p(e_h)$. In other words, the child graph is linked to its parent through several edges, traced between the neighbors of its assigned vertex in the parent and different vertices in the child graph. The assigned vertex $v_p(e_h)$ in these cases

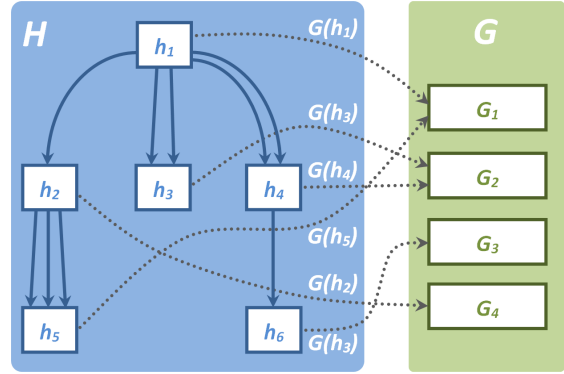


Figure 3: A diagram of a hierarchical CLI graph.

is not drawn, but replaced instead by the child graph in the final CLI.

By default, linking edges in our system are traced between the assigned vertex $v_p(e_h)$ (or its neighbors) and the vertex (or vertices) in the child graph that is closest to $v_p(e_h)$, while taking the position, rotation and scaling of $G(h_c)$ relative to $G(h_p)$ into account. However, our system also allows users to modify linking edges in order to connect them at specific vertices in the child graph.

5 CLI COMPUTATION

Once the overall hierarchical structure of the CLI has been designed, the next step is to compute the CLI itself. This section explains how to obtain CLIs from both a general or a hierarchical graph.

5.1 Single Graph to CLI

A CLI can be modeled as an Eulerian path in a given graph $G(V_G, E_G)$. For such a path to exist, it is necessary for G to be Eulerian or semi-Eulerian, i.e., it should contain at most two vertices of odd degree (Gross and Yellen, 2005). Assuming G is Eulerian or semi-Eulerian, an Eulerian path can be found in it by using Hierholzer's or Fleury's algorithm (Hierholzer and Wiener, 1873; Fleury, 1883).

In (Wong and Takahashi, 2011), we developed a semi-Eulerization technique that inserts, removes and duplicates graph edges systematically, in order to reduce the number of odd-vertices in the graph, while avoiding visual artifacts in our CLIs such as the excessive retracing of edges. We also proposed a modification to Fleury's algorithm that attempts to avoid unnatural changes in line curvature. Fleury's algorithm for semi-Eulerian graphs basically works as follows:

1. Set the current vertex u as one of the odd vertices.

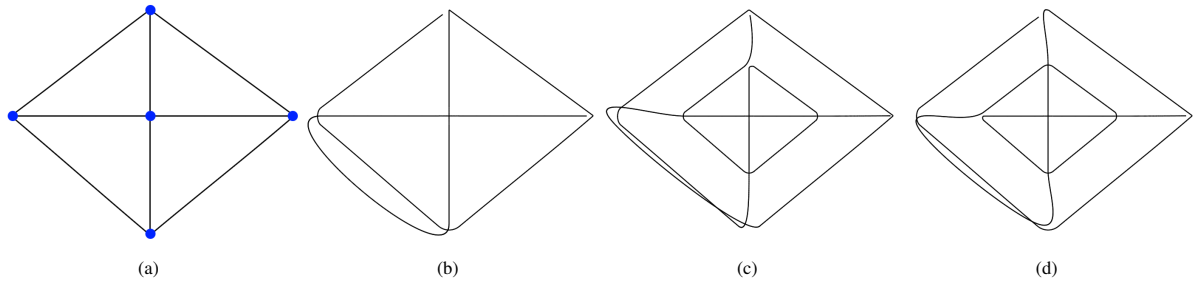


Figure 4: CLI coherence across hierarchical levels. (a) A diamond-shaped graph is converted into (b) a CLI. (c) A CLI generated after assigning the same graph to its central vertex. Although the new CLI has the same endpoints, the overall orientation followed by the line is different. (d) This orientation can be preserved as much as possible with our approach.

2. Select a non-bridge¹ edge $e = (u, v) \in E_G$.
3. Traverse to from u to v and remove e from G .
4. Repeat from Step 2 until no edges remain in G .
5. The Eulerian path is given by the order in which vertices were visited.

This algorithm was modified in Step 2 by matching the edges adjacent to u , in a way that minimizes the total difference in orientation between each pair of matched edges. Edge e is set as the edge matched to the previously traversed one, while enforcing the non-bridge condition during the matching process.

Arbitrary endpoints $p \in V_G$ and $q \in V_G$, can be specified for an Eulerian path by first inserting a fictitious edge (p, q) to G and then Eulerizing the graph until no odd vertices remain in G . Removing edge (p, q) will convert G from Eulerian to semi-Eulerian, after which the path can be found by applying our modified Fleury's algorithm.

5.2 Hierarchical Graph to CLI

Before creating a CLI from the hierarchical graph H , first we need to transform each basis graph accordingly. For each edge $(h_p, h_c) \in E_H$, the transformation matrix $\mathbf{A}(h_c)$ for a child graph $G(h_c)$ is given by

$$\mathbf{A}(h_c) = \mathbf{A}(h_p)\mathbf{T}(h_c)\mathbf{R}(h_c)\mathbf{S}(h_c) \quad (1)$$

where $\mathbf{T}(h_c)$, $\mathbf{R}(h_c)$ and $\mathbf{S}(h_c)$ are the translation, rotation and scaling matrices of $G(h_c)$ relative to $G(h_p)$.

Computing a CLI from H can then be achieved by combining all graphs into a single one by inserting linking edges accordingly, semi-Eulerizing the resulting graph, and finally computing an Eulerian path as described in Section 5.1. This approach, however, might introduce unwanted changes in the CLI as described in the next section.

¹A bridge is an edge whose removal would disconnect the graph into two different components.

5.3 Coherence Across Hierarchy Levels

Although a CLI can be obtained from a hierarchical graph by following the strategy in Section 5.2, this could result in changes to the overall structure of the CLI each time a graph is assigned or transformed relative to its parent as shown in Figure 4. This becomes an issue if we would like to generate several CLIs with the same orientation and endpoints, e.g., for making CLI-based keyframe animations. The problem is due to the process not considering the hierarchical relationships when computing the Eulerian path. This can be alleviated by taking the following steps:

1. Compute an Eulerian path in the root graph.
2. Modify each child graph according to this path.
3. Obtain a set of paths that collectively traverse through all edges of the child graph.
4. Insert each of these paths into the Eulerian path of the parent accordingly.

The path in Step 1 can be obtained by applying the process described in Section 5.1. The remaining steps are explained throughout the rest of this section.

5.3.1 Child Graph Modification

An Eulerian path of a parent graph $G(h_p)$ can traverse through a vertex $v \in V_{G(h_p)}$ any number of times in different directions. For example, if v has four neighbors $v_1, v_2, v_3, v_4 \in V_{G(h_p)}$, the path could first traverse through v from v_1 to v_3 and then from v_2 to v_4 . Let us suppose that $G(h_p)$ and $G(h_c)$ are related through an edge $e_h = (h_p, h_c) \in E_H$ with a multiple link relation, and that $v = v_p(e_h)$ in this example. This means that, if we replace v for $G(h_c)$, then the path should first enter $G(h_c)$ from a vertex $u_1 \in V_{G(h_c)}$, which is connected to v_1 through a linking edge, and then exit it through a vertex $u_3 \in V_{G(h_c)}$, which is connected to v_3 . The second time the path visits $G(h_c)$, it should enter it from a vertex u_2 and leave it through

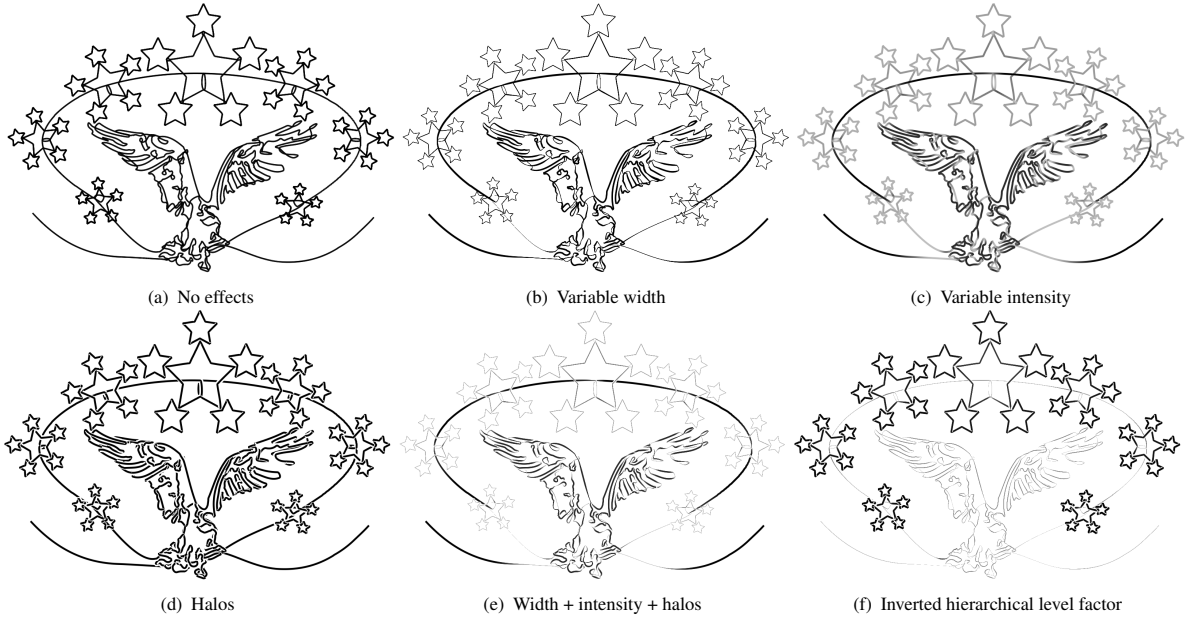


Figure 5: Hierarchy-based visual enhancements. (a) A CLI drawn with uniform thickness and color. The CLI can be rendered with (b) variable width, (c) variable intensity or (d) halos along the line. (e) These enhancements can be combined for obtaining CLIs with multiple effects. (f) The way in which the hierarchy influences each effect can be controlled freely.

a vertex u_4 . In this case, the way in which the path traverses through v defines a set of endpoint pairs $\mathcal{Q} = \{(u_1, u_3), (u_2, u_4)\}$ for graph $G(h_c)$.

If $G(h_c)$ has only one pair of endpoints (p, q) assigned to it, the graph is not modified. Otherwise, if two or more endpoint pairs $\mathcal{Q} = \{(p_1, q_1), \dots, (p_n, q_n)\}$ are assigned to $G(h_c)$, we perform a process similar to the one described in Section 5.1 for specifying arbitrary endpoints for the paths. We insert several fictitious edges (p_i, q_i) into $G(h_c)$, Eulerize the graph, and then remove all edges (p_i, q_i) from $G(h_c)$, thus making the vertices in \mathcal{Q} the only odd vertices of the graph.

5.3.2 Covering a Graph with a Set of Paths

The goal now is to compute a set of paths $\mathbf{P} = \{P(p_1, q_1), \dots, P(p_n, q_n)\}$ for each $(p_i, q_i) \in \mathcal{Q}$, so that \mathbf{P} covers all edges in $G(h_c)$. We employ a combined version of Fleury's and Hierholzer's algorithm in order to achieve this. Hierholzer's algorithm for a semi-Eulerian graph $G(V, E)$ consists in the following (Hierholzer and Wiener, 1873):

1. Obtain a path $P(s, t)$ between the two vertices of odd degree $s, t \in V$ in G .
2. For a vertex $v \in P(s, t)$ with adjacent edges $(u, v) \notin P(s, t)$, compute a cycle $C(v)$ by starting at v and traversing only through edges not included in $P(s, t)$ until returning to v .
3. Insert $C(v)$ into $P(s, t)$ at vertex $v \in P(s, t)$.

4. Return to Step 2 until $P(s, t)$ covers all edges in G .

In other words, a path between the two odd vertices is computed first, and then the Eulerian path is finished by appending cycles to the path until it contains all edges in G . The algorithm can be modified for our purposes in the following manner:

1. Copy $G(h_c)$ into a graph $G'(h_c)$.
2. For each $(p_i, q_i) \in \mathcal{Q}$, insert a set of directed edges $\{(q_i, p_j), (q_i, q_j) \mid i \neq j\}$ in $G(h_c)$.
3. Find a path $P(p_i, q_i)$ by partially applying the extended Fleury's algorithm (Section 5.1) from p_i until reaching q_i in $G(h_c)$.
4. Remove all edges $(u, v) \in P(p_i, q_i)$ from $G'(h_c)$ whose removal will not disconnect $G'(h_c)$.
5. Copy $G'(h_c)$ into $G(h_c)$.
6. Repeat from Step 2 for the next $(p_i, q_i) \in \mathcal{Q}$.
7. For a vertex $v \in P(p_i, q_i)$ with adjacent edges $(u, v) \notin \mathbf{P}$, find a cycle $C(v)$ by using the extended Fleury's algorithm from v and traversing through edges not included in \mathbf{P} until returning to v .
8. Insert $C(v)$ into $P(p_i, q_i)$ at vertex v .
9. Repeat from Step 7 for different $P(p_i, q_i) \in \mathbf{P}$ until \mathbf{P} covers all edges in $G(h_c)$.

Essentially, we have applied Hierholzer's algorithm for multiple pairs of odd vertices, and replaced both the initial path and subsequent cycle computations by the extended Fleury's algorithm, so that the

final path tends to avoid drastic changes in curvature. The insertion of directed edges in Step 2 is performed in order to fulfill the non-bridge condition during the edge selection step of Fleury's algorithm. Note these edges are not inserted in $G'(h_c)$, whose purpose is to ensure the graph connectivity in the next iteration.

5.3.3 Inserting the Paths into the Eulerian Path

The next step is to insert the set of computed paths for $G(h_c)$ into the Eulerian path of its parent graph $G(h_p)$. This is done by replacing all instances of $v_p(e_h)$ in the Eulerian path for the appropriate computed paths. In this way, we can assign several child graphs to a parent graph, without changing the overall structure of the final CLI.

6 CLI RENDERING

Several strategies for rendering CLIs were proposed in (Wong and Takahashi, 2011), such as trimming the line segments of the Eulerian path, the inclusion of curl and cusp features, among others. We extend this work, by providing visual CLI enhancements based on the hierarchical structure of our CLIs.

More specifically, we allow users to vary the thickness and intensity of the line according to the hierarchy. Edges of graphs at higher levels can be rendered thicker (Figure 5(b)) and darker (Figure 5(c)) than those at lower levels, or vice-versa. In order to achieve this, a hierarchical value is first assigned to each point in the CLI, based on the level of its basis graph in the hierarchy, and then width and intensity values for each point are computed according to it. These values are interpolated along the neighborhood of points in the CLI where the hierarchical level changes, in order to achieve smooth transitions in the thickness and intensity of the line. A triangle strip is then created by computing points separated by half of the specified width from each of the CLI points at directions perpendicular to the line orientation, while modulating the intensity of the line based on the previously computed values.

We also incorporate depth-dependent halos (Everts et al., 2009) in our CLIs, allowing the viewer to better perceive the self-intersections in the line (Figure 5(d)). The depth of each point contained in the CLI is given by its hierarchical level, thus portraying lines at higher hierarchies as if traced on top of those at lower levels. Multiple visual enhancements can be applied to any of our CLIs, as shown in Figure 5(e), and the way in which each effect is influenced by the hierarchy of the CLI can be adjusted as well, allowing

Table 1: Computation times of CLI generation.

	Figure 6(c)	Figure 6(d)	Figure 7(b)
Path Computations ²	0.167s	1.260s	0.762s
Path Mergings ³	0.123s	0.331s	0.055s
Rendering	0.108s	0.488s	0.303s
Total	0.398s	2.079s	1.120s
Number of Graphs	11	26	4
Total Edge Count	292	4514	3094

² Time spent in semi-Eulerization and Eulerian path computations.

³ Time spent in merging paths of child graphs with the Eulerian paths of their parents.

us to emphasize edges at higher or lower levels as we like (Figure 5(f)). Linking edges in our approach are drawn as Catmull-Rom splines (Catmull and Rom, 1974), and are rendered thinner, lighter and at lower depths than other edges, in order to keep them from standing out in the illustration.

7 RESULTS AND DISCUSSION

Our prototype system was implemented in C++ on an Intel Core 2 Duo E6550 2.33 Ghz CPU with 2 GB of RAM. Table 1 summarizes the computation time statistics for generating some of the CLI examples presented in this paper by using this setup. As can be seen, generating a CLI takes just a few seconds, even for hierarchical graphs that contain a large total number of edges. Several results of our approach can be seen in Figures 1, 5, 6 and 7.

Figures 5(a), 6(a), 6(b) and 7(a) portray CLIs with uniform thickness and color, while Figures 5(e), 6(c), 6(d) and 7(b) show their respective versions after applying the hierarchy-based enhancing effects introduced in Section 6. As can be seen, these effects greatly improve the visualization and aesthetics of our CLIs. This is better appreciated in Figure 6(d), where the musical note on top of the tree is clearly visible and the depth perception of the grass is enhanced, as opposed to its regular CLI version shown in Figure 6(b). The same can be said of Figure 7(b), in which the buildings give the illusion of being located far away, while the bridge gives the impression of being placed nearer to the viewer. Our hierarchical CLIs are good for designing logos such as the one shown in Figures 6(a) and 6(c), and can also be used for portraying text as a single line (Figure 7(c)).

8 CONCLUSIONS

A framework for designing complex continuous line illustrations that portray different objects with a single line has been proposed in this paper. We employed an approach based on the use of a hierarchical graph

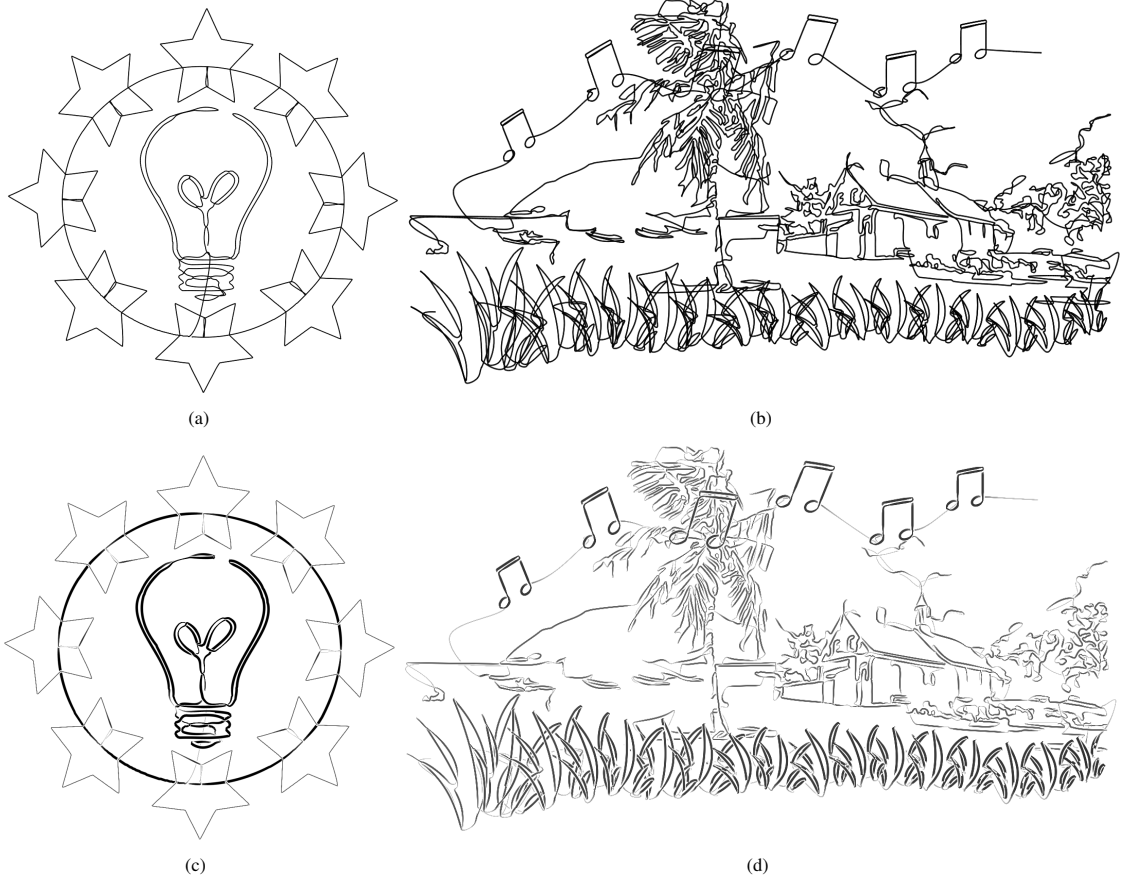


Figure 6: Hierarchical CLI results generated with our approach.

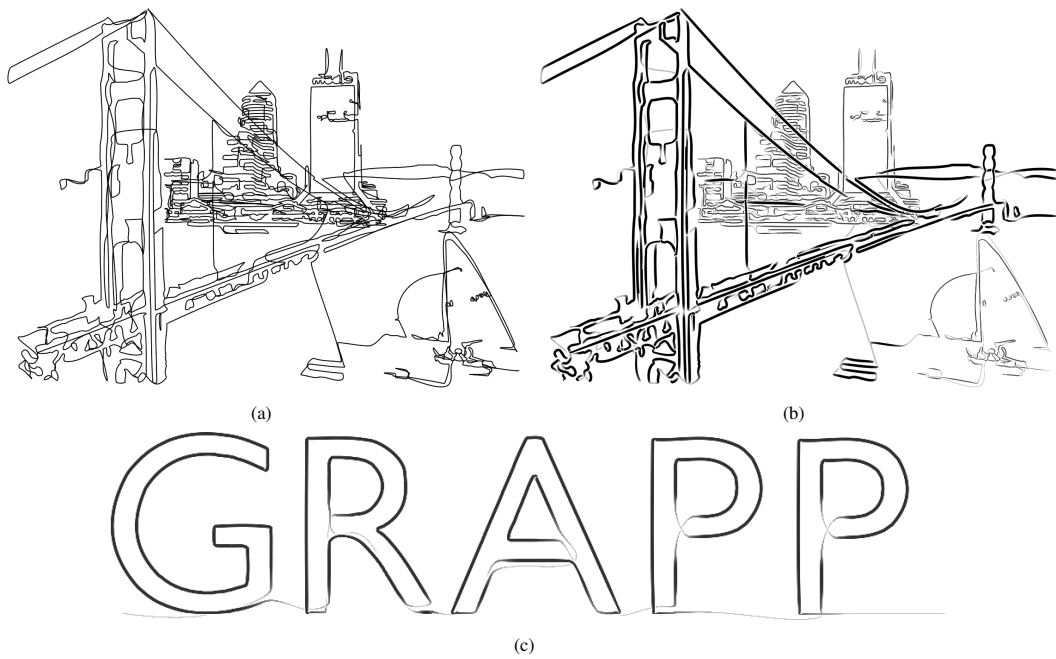


Figure 7: More hierarchical CLI results.

that models the relationships between different basis graphs, which represent the objects portrayed in the final illustration. We have given detailed explanation as to how to obtain a CLI from one of such hierarchical graphs, while at the same time preserving the coherence of the CLI independently of the number of graphs specified in the hierarchical graph structure. Visual enhancements based on the hierarchy of the CLI can also be achieved in our approach.

Our CLIs often seem to contain either too few or too many features in them, due to the image-to-graph conversion process employed in our approach being based on edge detection techniques, which are prone to subdetection and overdetection of edges. Although our system allows users to modify the set of detected edges prior to generating a graph, this is a particularly daunting task for a large number of edges. The amount of line thickness variation supported by our system is also limited, resulting in visual artifacts appearing along the line as the thickness increases. This could be alleviated to some extent by applying techniques for avoiding and correcting folds in skeletal strokes to our CLIs (Hsu et al., 1993; Asente, 2010).

As future work, we would like to apply this approach for generating CLI-based animations, as well as to incorporate ideas from previous works (Bosch and Herman, 2004; Kaplan and Bosch, 2005; Wong and Takahashi, 2009) for producing illustrations that portray both the contours and the shading of the image. We also would like to explore ways to effectively include color into our illustrations, as well as to allow the placement of text along the line (Surazhsky and Elber, 2000; Maharik et al., 2011).

REFERENCES

- Asente, P. J. (2010). Folding avoidance in skeletal strokes. In *Proceedings of the Seventh Sketch-Based Interfaces and Modeling Symposium*, pages 33–40. Eurographics Association.
- Bosch, R. and Herman, A. (2004). Continuous line drawings via the traveling salesman problem. *Operations Research Letters*, 32(4):302–303.
- Catmull, E. and Rom, R. (1974). A class of local interpolating splines. In *Computer Aided Geometric Design*, pages 317–326.
- Everts, M. H., Bekker, H., Roerdink, J. B. T. M., and Isenberg, T. (2009). Depth-dependent halos: Illustrative rendering of dense line data. *IEEE Transactions on Visualization and Computer Graphics*, 15(6):1299–1306.
- Fleury, M. (1883). Deux problemes de geometrie de situation. *Journal de Mathematiques Elementaires*, pages 257–261.
- Fritz, L. L. (2001). *250 Continuous-Line Quilting Designs for Hand, Machine & Long-Arm Quilters*. C&T Publishing, Inc.
- Gross, J. L. and Yellen, J. (2005). *Graph Theory and Its Applications, Second Edition (Discrete Mathematics and Its Applications)*. Chapman & Hall/CRC.
- Hierholzer, C. and Wiener, C. (1873). Ueber die Möglichkeit, einen Linienzug ohne Wiederholung und ohne Unterbrechung zu umfahren. *Mathematische Annalen*, 6(1):30–32.
- Hsu, S. C., Lee, I. H. H., and Wiseman, N. E. (1993). Skeletal strokes. In *Proceedings of the 6th annual ACM symposium on User interface software and technology*, pages 197–206. ACM.
- Kaplan, C. S. and Bosch, R. (2005). TSP Art. In *Proceedings of Bridges 2005, Mathematical Connections in Art, Music and Science*, pages 301–308.
- Lindsay, R. A. (2010). Rachel Ann Lindsay - illustrator. <http://www.rachelannlindsay.com/>.
- Lohman, S. (2009). LineArtGallery.com. <http://www.lineartgallery.com/>.
- Maharik, R., Bessmeltsev, M., Sheffer, A., Shamir, A., and Carr, N. (2011). Digital micrography. *ACM Transactions on Graphics*, 30(4):100:1–100:12.
- Morales, J. E. (2005). Virtual Mo. <http://www.virtualmo.com/>.
- Nicolaides, K. (1990). *The Natural Way to Draw*. Houghton Mifflin Company, Boston, Massachusetts, USA.
- Pedersen, H. and Singh, K. (2006). Organic labyrinths and mazes. In *NPAP '06: Proceedings of the 4th international symposium on Non-photorealistic animation and rendering*, pages 79–86. ACM.
- Sable, P. (2009). Single line artwork by Pamela Sable. <http://www.pameline.com/>.
- Slater, G. (2001). Geoff Slater: Contemporary artist. <http://www.geoffslater.com/>.
- Surazhsky, T. and Elber, G. (2000). Arbitrary precise orientation specification for layout of text. In *Proceedings of the 8th Pacific Conference on Computer Graphics and Applications*, pages 80–86. IEEE Computer Society.
- Wong, F. J. and Takahashi, S. (2009). Flow-based automatic generation of hybrid picture mazes. *Computer Graphics Forum*, 28(7):1975–1984.
- Wong, F. J. and Takahashi, S. (2011). A graph-based approach to continuous line illustrations with variable levels of detail. *Computer Graphics Forum*, 30(7):1931–1939.